

Material contacts under cyclic compression, studied in real time by electrical resistance measurement

XIANGCHENG LUO, D. D. L. CHUNG

Composite Materials Research Laboratory, State University of New York at Buffalo, Buffalo, NY 14260-4400, USA

E-mail: ddlchung@acsu.buffalo.edu

Contacts of similar materials under cyclic compression below the yield stress were studied in real time by measurement of the contact electrical resistance. For all materials studied (steel, aluminum, copper, polymer and cement mortar), the contact resistance decreased upon loading in every load cycle. The resistance at the minimum stress of a cycle decreased upon load cycling for steel (at a sufficiently high stress amplitude), polymer-matrix composite and mortar due to plastic deformation at asperities, but increased upon cycling for aluminum and copper, probably due to surface oxidation and/or strain hardening. For steel and aluminum, the resistance at the maximum stress of a cycle increased upon load cycling, probably due to oxidation and/or strain hardening, and it took more stress for the resistance to decrease in a cycle as cycling progressed, probably due to strain hardening. For the polymer (thermoplastic), it took less stress for the resistance to decrease in a cycle as cycling progressed, probably due to enhancement of the molecular orientation perpendicular to the stress. For the mortar, the minimum resistance at the maximum stress increased slightly as cycling progressed, probably due to debris generation. © 2000 Kluwer Academic Publishers

1. Introduction

Different pieces of materials, whether similar or dissimilar materials, can be brought into direct contact without bonding at the interface. Such contacts are commonly maintained by using a static pressure, so they are called pressure contacts. The static pressure may be an externally applied pressure or simply pressure due to the weight of the top piece on the bottom piece of the assembly. Examples of such contacts are (i) the contact between a fastener (such as a rivet) and a component to be fastened (such as a plate), (ii) the contact between a concrete slab and a concrete column in a bridge structure, and (iii) the contact between a metal clip and a metal wire, as encountered in making an electrical connection.

Contacts are often subjected to a dynamic pressure, which can be due to fastening (loading) and unfastening (unloading) in example (i), due to live loads from vehicles traveling on the bridge in example (ii), and due to clipping (loading/connecting) and unclipping (unloading/disconnecting) in example (iii). The dynamic loading is commonly assumed to have no irreversible effect on the interface or the contact quality due to the low load level involved. However, this assumption may not be correct, since the mating surfaces are usually not perfectly smooth and the stress encountered by the asperities at the interface is much larger than the overall applied stress. The high local stress may cause local

plastic deformation or even local debris formation, thus causing irreversible effects to the contact, even though the applied stress is below the yield stress. Therefore, study of contacts during dynamic compression is of practical and fundamental interest, though it has received little prior attention. On the other hand, much prior attention has been given to contacts during dynamic shear, due to the relevance to wear and abrasion. Dynamic compression is expected to cause more subtle effects than dynamic shear, since shear is associated with a tearing action.

Wear or abrasion involves subjecting each point of a surface to dynamic shear. Studies of wear or abrasion are commonly conducted by monitoring the effect over an area rather than that at a fixed point. For example, in wear testing using the pin-on-disk configuration, the tip of the pin is continuously moved against the surface of the disk, so that different points on the disk are subjected to stress at different times and the effect of dynamic shear and the stress variation within a cycle of dynamic shear at a particular point of the surface are not monitored. Even if the effect of wear or abrasion is monitored in real time, say by measuring the contact electrical resistance at the sliding contact between the pin and the disk, the monitoring does not allow correlation of the effect (say the electrical resistance) at a point with the dynamic stress at the point within a stress cycle. (The dynamic stress is to be distinguished

from the stress amplitude.) This difficulty with wear or abrasion studies stems from the fact that wear or abrasion involves one element sliding against another, so that different points in a contact are not subjected to dynamic stress in an in-phase manner. In contrast, dynamic compression does not involve sliding, so that each point in a contact is subjected to dynamic compression in an in-phase manner, i.e., all points experience the maximum compressive stress in a cycle simultaneously and all points experience the minimum stress in a cycle simultaneously. As a result, correlation is possible between the effect (say the contact electrical resistance at the contact) and the dynamic stress during dynamic loading. This correlation allows identification of the point in a stress cycle at which certain effect occurs, and moreover allows distinction between reversible effects (effects, such as elastic deformation, which vanish upon unloading) and irreversible effects (effects, such as plastic deformation, which remain upon unloading). Therefore, by studying the effect of dynamic compression rather than dynamic shear, this paper provides new information on the dynamic mechanical behavior of contacts, i.e., the behavior of contacts under dynamic loading.

The dynamic mechanical behavior of monolithic materials has received much attention, partly because of its relevance to vibration damping, which is valuable to structures. However, the dynamic mechanical behavior of materials contacts has received little previous attention (except in relation to wear or abrasion). This paper is a study of the dynamic mechanical behavior of contacts between various identical materials, i.e., between metal (e.g., steel, aluminum and copper) elements, between polymer elements, and between ceramic (i.e., concrete that is already cured) elements. The differences in mechanical properties and oxidation tendency among metals, polymers and ceramics results in significant differences in the dynamic mechanical behavior of the contacts involving these materials. Contacts between dissimilar materials are not addressed in this paper. The effects of loading frequency and temperature on the dynamic mechanical behavior are also not addressed. There is much room for future work.

The technique used in this work for studying the dynamic mechanical behavior of contacts is contact electrical resistance measurement during cyclic compression below the yield stress. (Cyclic loading is a simple type of dynamic loading in which the stress amplitude and frequency are kept constant.) It involves simultaneous electrical and mechanical measurements. The technique requires that the elements in contact are electrically conducting. Metals and concrete are conducting, but polymers are mostly not conducting. In order to study polymer contacts, we used a carbon fiber thermoplastic-matrix composite instead of the polymer by itself. The carbon fibers are electrically conducting, thereby rendering the composite conducting. By orienting the continuous fibers parallel to the plane of the contact, the mechanical properties of the composite in the compressive stress direction (direction perpendicular to the plane of the contact) are dominated by the polymer matrix. In spite of the orientation of the fibers, the composite is conducting even in the compressive

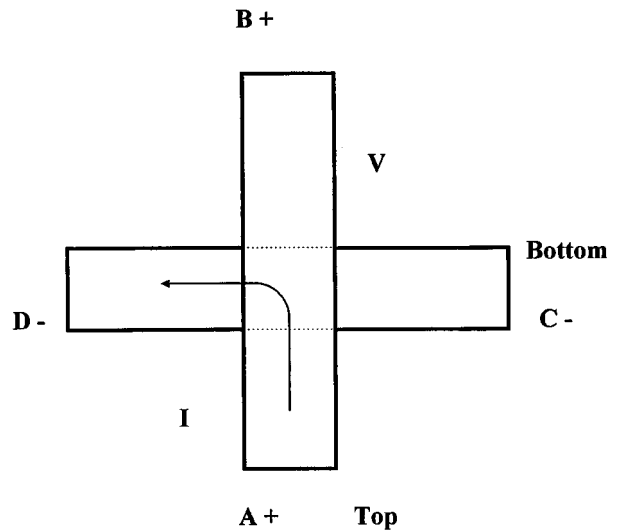


Figure 1 Metal and polymer test configuration.

stress direction. This is because direct contacts between “parallel” fibers occur at some points along the length of a fiber.

The contact resistance of the interface between contacting elements can be conveniently measured by using the elements as electrical leads – two for passing current and two for voltage measurement (i.e., the four-probe method), as provided by two elements (beams) that overlap at 90° (Fig. 1). The volume resistance of each lead was negligible compared to the contact resistance of the junction, so the measured electrical resistance was the contact resistance. The contact resistance multiplied by the junction area gives the contact resistivity, which is independent of the junction area and describes the structure of the interface.

Contact electrical resistance measurement has been previously used to study the interface between laminae in a carbon fiber polymer-matrix composite laminate [1] and to study the joint obtained between thermoplastic elements by autohesion [2, 3]. In the field of concrete, contact electrical resistance measurement has been previously used to study the joint between old and new concrete [4], as this joint is relevant to the repair of concrete structures. It has also been used to study the interface between concrete and steel [5, 6] and that between cement paste and carbon fiber [7, 8].

2. Experimental methods

2.1. Electrical and mechanical measurements

Two rectangular strips of the same material were allowed to overlap at 90° to form a nearly square junction, as illustrated in Fig. 1 (for metals and polymer) and in Fig. 2 (for cement mortar). The junction was the joint under study. Uniaxial cyclic compression was applied at the junction in the direction perpendicular to the junction, using a screw-action mechanical testing system (Sintech 2/D, Sintech, Research Triangle Park, NC), while the contact electrical resistivity of the junction was measured. The crosshead displacement during load cycling was typically up to 3 μm.

For mortar, polymer and aluminum samples, copper wires were applied around the strips together with silver

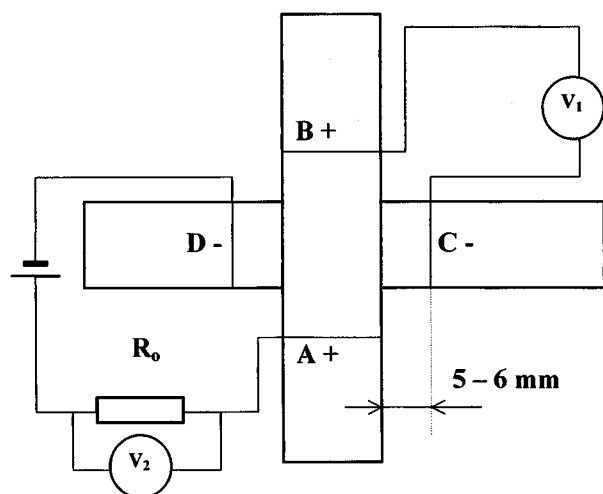


Figure 2 Mortar test configuration.

paint to serve as electrical contacts. For steel and copper samples, copper wires were soldered on the samples to serve as electrical contacts. To measure the contact resistivity at the junction, a Keithley 2002 multimeter was used for metals and polymer samples (Fig. 1). For mortar samples, a DC power source and a standard resistor R_0 with a resistance of 30.4 M Ω were used, due to the high contact resistance involved (Fig. 2). In all cases (Figs 1 and 2), a DC current was applied from A to D, so that the current traveled down the junction from the top strip to the bottom strip. In Fig. 2, the voltage between B and C (V_1) as well as the voltage on the standard resistor (V_2) were measured using the Keithley 2002 multimeter. V_1 was the voltage across the junction between the top and bottom strips and V_2 was used to obtain the current passing from A to D. The use of two current probes (A and D) and two voltage probes (B and C) corresponded to the four-probe method of resistance measurement. The voltage divided by the current yielded the contact resistance of the junction.

2.2. Materials

Steel (low carbon steel), aluminum, copper, polymer (Nylon-6) and cement (Portland cement) were used in the study of the contact between identical materials under cyclic compression. Mortar is different from concrete in that mortar has a fine aggregate but no coarse aggregate, whereas concrete has both fine and coarse aggregates. Mortar rather than concrete was used in this study because of the small sample size involved. Nevertheless, the science of the contact should be similar for mortar and concrete.

The steel used was low carbon steel sheet that had been mechanically polished by 600-grit sandpaper, in which the average abrasive SiC particle size is 25 μm . Two identical rectangular strips of steel (20.0 \times 11.7 \times 6.0 mm) were allowed to overlap at 90° to form a square junction (11.7 \times 11.7 mm), as illustrated in Fig. 1.

The as-received aluminum and copper foils were cut into rectangular strips of length around 60 mm and width between 5.8 and 6.8 mm. The thicknesses of copper and aluminum foils were 0.025 and 0.050 mm, respectively. Two strips of the same material were al-

lowed to overlap at 90° to form a nearly square junction (5.8–6.2 mm \times 6.0–6.8 mm), as illustrated in Fig. 1.

The steel used was in sheet form, whereas the aluminum and copper used were in foil form. The foils were low in weight and consequently the upper strip of the junction provided little pressure to the bottom strip, compared to the case of the strips being in sheet form. As a result, the contact resistance at a zero applied stress for aluminum and copper was less reproducible than that for steel. To alleviate this problem, a non-zero minimum stress was used during load cycling for aluminum and copper whereas a zero minimum stress was used for steel. At any rate, the minimum stress of 0.4 MPa for aluminum and that of 0.3 MPa for copper were quite close to zero.

The thermoplastic polymer was Nylon-6 (PA) in the form of unidirectional carbon-fiber (CF) prepreg supplied by Quadrax Corp. (Portsmouth, Rhode Island; QNC 4162). The fibers were 34-700 from Grafil, Inc. (Sacramento, California). The fiber diameter was 6.9 μm . The fiber weight fraction in the prepreg was 62%. The glass transition temperature (T_g) was 40–60°C and the melting temperature (T_m) was 220°C for the Nylon-6 matrix. The prepreg thickness was 250 μm . The prepreg strip was of length about 72 mm and of width between 8.2 and 11.1 mm. Two strips were allowed to overlap at 90° to form a rectangular junction (8.2–10.4 \times 9.5–11.1 mm), as illustrated in Fig. 1.

The cement used was portland cement (Type I) from Lafarge Corp. (Southfield, MI). The fine aggregate used for mortars was natural sand (all passing #4 U.S. sieve, 99.9% SiO₂); the particle size analysis of the sand is shown in Fig. 1 of Ref. 9; no coarse aggregate was used, and the sand/cement ratio was 1.0. The water/cement ratio was 0.35. A water-reducing agent (TAMON SN, Rohm and Haas Co., Philadelphia, PA; sodium salt of a condensed naphthalenesulphonic acid) was used in the amount 1% of the cement weight. All ingredients were mixed in a Hobart mixer with a flat beater. After pouring into molds, an external vibrator was used to facilitate compaction and decrease the amount of air bubbles. The samples were demolded after 24 h and then cured in a moist room (relative humidity = 100%) for 28 days. The final sizes of the mortar samples (strips) were 90.0 \times 14.0 \times 13.3 mm and 95.0 \times 14.2 \times 13.9 mm. The surfaces of mortar strips had been mechanically polished by 600-grit sandpaper. Two mortar strips were allowed to overlap at 90° to form a nearly square junction (13.9 \times 13.3 mm), as illustrated in Fig. 2.

3. Results and discussion

3.1. Metals

Fig. 3 shows the variation in resistance and stress during compressive cyclic loading with a maximum stress of 20.0 MPa and a minimum stress of zero for steel. In every cycle, the resistance decreased as the compressive stress increased, such that the maximum stress corresponded to the minimum resistance and the minimum stress corresponded to the maximum resistance. Similar resistance variations were found for aluminum (Fig. 4) with a maximum stress of 6.3 MPa and for copper (Fig. 5) with a maximum stress of 5.7 MPa. The

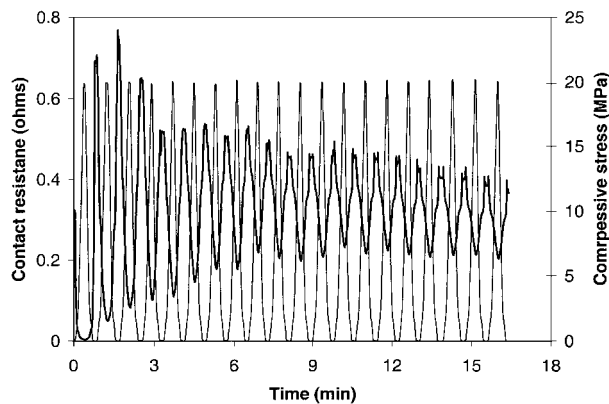


Figure 3 Variation of contact resistance (thick curve) and stress (thin curve) for steel during cyclic compression at a maximum stress of 20.0 MPa and a minimum stress of zero.

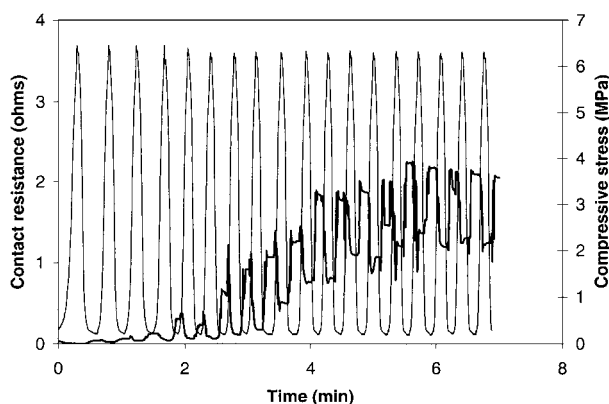


Figure 4 Variation of contact resistance (thick curve) and stress (thin curve) for aluminum during cyclic compression at a maximum stress of 6.3 MPa and a minimum stress of 0.4 MPa.

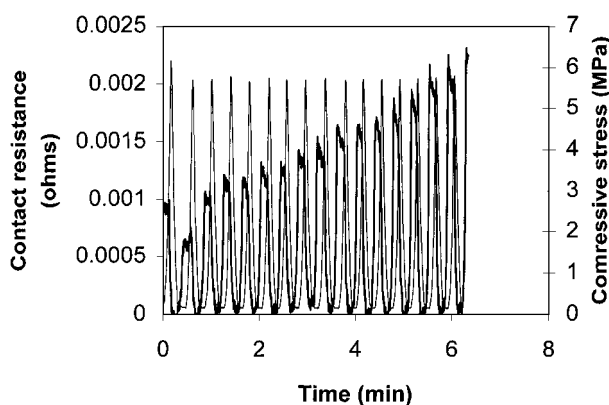


Figure 5 Variation of contact resistance (thick curve) and stress (thin curve) for copper during cyclic compression at a maximum stress of 5.7 MPa and a minimum stress of 0.3 MPa.

maximum stress of 20, 6.3 and 5.7 MPa for steel, aluminum and copper respectively was much lower than the corresponding yield strength, which was 300 MPa for steel (determined by compressive testing in this work), 28 MPa for aluminum [10] and 69 MPa for copper [10]. Due to the roughness on the steel, aluminum and copper surfaces, the local stress at the asperities was much higher than the applied stress and could cause local elastic or even plastic deformation. As a result, upon loading the surface was flattened to a certain extent, and

consequently the resistance decreased upon loading in each cycle for all materials.

The contact resistance at the maximum stress of each cycle increased upon cycling, for steel and aluminum at least, probably partly due to the oxidation at the fresh surface created by the deformation and partly due to the strain hardening induced by the plastic deformation. (The oxide is essentially not conducting and the strain hardening tends to increase the volume resistivity.) This trend was not observed for copper, probably due to the exceptionally low contact resistance for copper throughout the cycling (as expected from the low volume electrical resistivity of copper compared to steel or aluminum) and that the oxide layer on copper fractured upon loading (in contrast to the protective oxide layer on aluminum).

For steel, due to the irreversible contact area increase resulting from plastic deformation, the resistance at the minimum stress decreased cycle by cycle from the third cycle onward, though the decrease diminished as cycling progressed due to the limit of the extent of plastic deformation. However, for aluminum and copper, the resistance at the minimum stress increased with cycling throughout the cycling, probably due to the effect of surface oxidation and/or strain hardening overshadowing the effect of surface flattening. For steel, the resistance at the minimum stress increased during the first two cycles, probably due to the surface oxidation that accompanied plastic deformation.

For steel, the resistance curve became sharper and sharper at its minimum in each cycle as cycling progressed (Fig. 6), probably due to strain hardening and the consequent increase in the stress required for a substantial resistance decrease within a cycle. This was similarly observed for aluminum (but not for copper) after the first few cycles (Fig. 4). The negative observation for copper was for the same reason as that given above for the absence of an increase in the minimum resistance of a cycle as cycling progressed.

At a lower stress amplitude (a maximum stress of 13.2 MPa and a minimum stress of zero) for steel (Fig. 7), the maximum resistance within a cycle increased with cycling and the resistance curve at its minimum remained blunt throughout the cycling. These characteristics are attributed to the smaller extent of

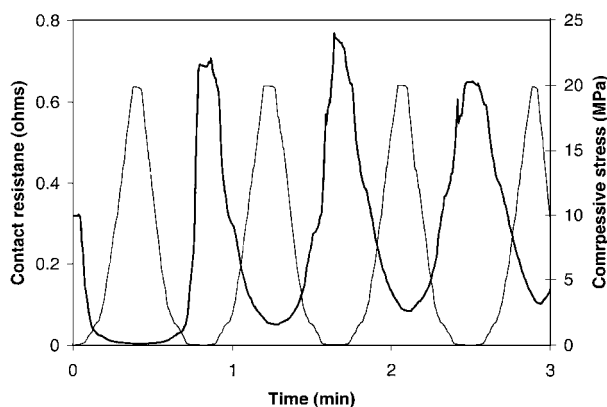


Figure 6 Variation of contact resistance (thick curve) and stress (thin curve) for steel during cyclic compression at a maximum stress of 20.0 MPa for the first few cycles.

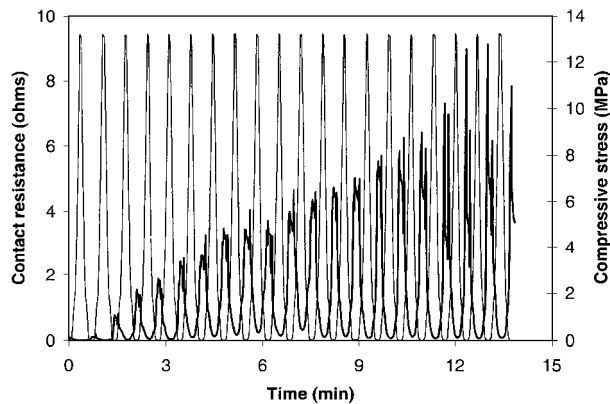


Figure 7 Variation of contact resistance (thick curve) and stress (thin curve) for steel during cyclic compression at a maximum stress of 13.2 MPa and a minimum stress of zero.

plastic deformation at the lower stress amplitude and the consequent gradual build-up of strain hardening and surface oxidation as cycling progressed. At a higher stress amplitude (Fig. 3), this build-up occurred mainly during the first two cycles.

3.2. Polymer

Fig. 8 shows the variation in resistance and stress during cyclic compressive loading at a stress amplitude of 0.8 MPa (a maximum stress of 0.8 MPa and a minimum stress of zero). Although the applied stress amplitude of 0.8 MPa was much less than the 1% offset yield stress (83 MPa [11]), due to the roughness at the interface, the local stress could be much higher than the applied stress. As a result, local plastic deformation could occur. The minimum resistance (at the maximum stress) decreased upon cycling. So did the maximum resistance (at the minimum stress). Both effects are attributed to plastic deformation.

Within the first cycle, the resistance curve was sharp at the maximum stress region. The resistance curve at the maximum stress region became increasingly blunt as cycling progressed (Fig. 9). This means that it took less and less stress for the resistance to decrease significantly as cycling progressed. This trend is opposite to that for steel (Fig. 6) and aluminum (Fig. 4), for which the resistance curve at the maximum stress region became increasingly sharp as cycling progressed. Since during loading there is no electrical property change in

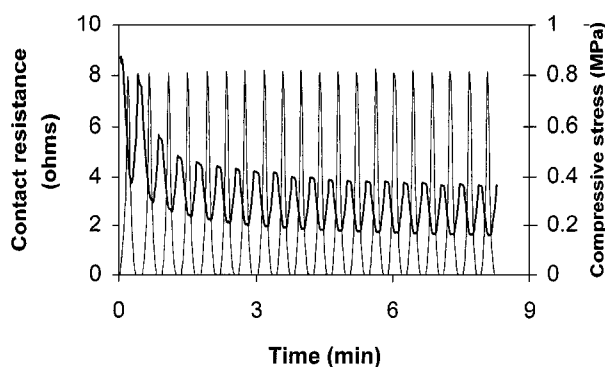


Figure 8 Variation of contact resistance (thick curve) and stress (thin curve) for polymer during cyclic compression at a maximum stress of 0.8 MPa and a minimum stress of zero.

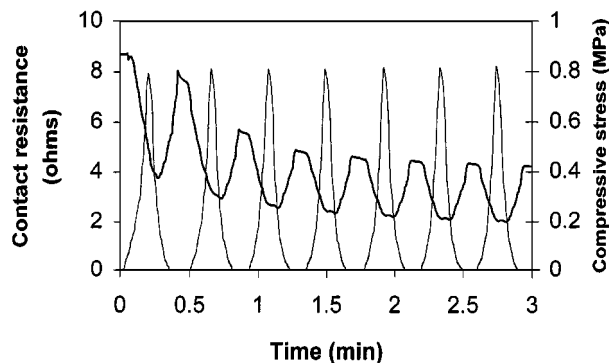


Figure 9 Variation of contact resistance (thick curve) and stress (thin curve) for polymer during cyclic compression at a maximum stress of 0.8 MPa for the first 7 cycles.

the carbon fiber, which is the component responsible for the electrical conduction, the electrical resistance change is attributed to the change in the extent of contact between fibers on both sides of the interface. A lower contact resistance at the interface means more contact between the fibers across the interface. The compressive stress probably made the polymer molecules orient preferentially perpendicular to the stress direction. This orientation would weaken the mechanical property of the matrix in the stress direction, especially near the interface. In other words, the compressive loading probably softened the matrix in the stress direction gradually as cycling progressed. The softening would make it take less stress for deformation and thus less stress for contact of fibers across the interface. This is believed to be why the resistance curve became blunter as cycling progressed. The gradual decrease of the resistance at both maximum and minimum stresses is due to the surface of the prepreg becoming flatter as cycling progressed. After about ten loading cycles, the resistance curve leveled off, probably due to the limit of the extent of flattening the surface of the prepreg.

3.3. Mortar

Fig. 10 shows the variation in resistance and stress during cyclic compressive loading at a stress amplitude of 5.0 MPa (a maximum stress of 5.0 MPa and a minimum stress of zero). The compressive strength of the

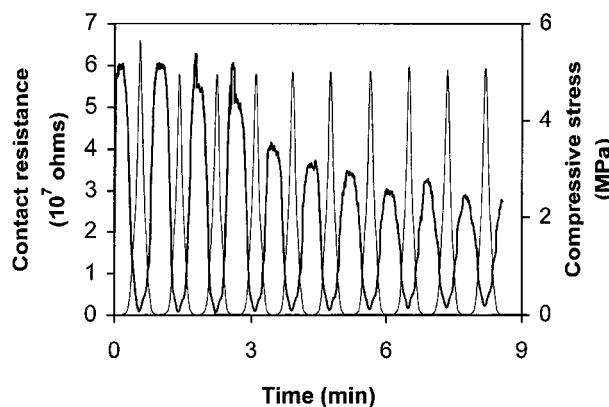


Figure 10 Variation of contact resistance (thick curve) and stress (thin curve) for mortar during cyclic compression at a maximum stress of 5.0 MPa and a minimum stress of zero.

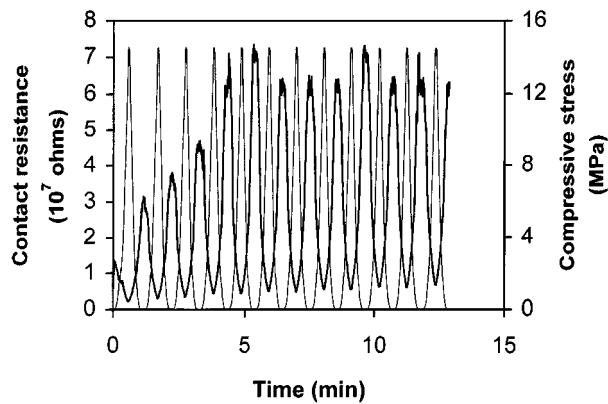


Figure 11 Variation of contact resistance (thick curve) and stress (thin curve) for mortar during cyclic compression at a maximum stress of 15.0 MPa and a minimum stress of zero.

mortar was 64 ± 2 MPa, as determined by compressive testing of $51 \times 51 \times 51$ mm ($2 \times 2 \times 2$ in) cubes. The stress-strain curve was a straight line up to failure. The minimum resistance (at the maximum stress) increased slightly with cycling, but the maximum resistance (at the minimum stress) decreased with cycling. Again, the local plastic deformation created more contact area, thus causing the resistance upon unloading to decrease with cycling. On the other hand, due to the brittleness of the mortar, the compressive loading probably caused fracture at some of the asperities at the interface, thereby generating debris, which increased the contact resistance upon loading. After about seven loading cycles, the maximum resistance (at the minimum stress) leveled off, due to the limit of the extent of the plastic deformation at the interface. However, the slight increase of the minimum resistance upon loading persisted, probably due to the continued generation of debris as cycling progressed. At a higher stress amplitude (a maximum stress of 15 MPa and a minimum stress of zero, Fig. 11), the minimum resistance increased more significantly with cycling. This is probably due to the more significant debris generation at the higher stress amplitude. Moreover, the maximum resistance (at the minimum stress) increased in the first four cycles, probably due to the effect of debris generation overshadowing the effect of the flattening of the asperities. After four cycles, the maximum resistance essentially leveled off, probably due to the limit of the extent of the debris generation for this stress amplitude.

3.4. Comparison among materials

For all materials tested, the contact resistance decreased as the compressive stress increased within a cycle and the contact resistance increased as the compressive stress decreased within a cycle. This is due to the surface roughness and the consequent deformation at the asperities. Hence, more contact area was created upon loading. For all materials tested, the contact resistance depended on the loading history.

Compared with metals (steel and aluminum) and polymer, a significant difference of mortar was that the resistance curve within a cycle essentially did not change its sharpness at the maximum stress. For the

polymer, the sharpness decreased with cycling, probably due to matrix softening. For metals (steel and aluminum), the sharpness increased, probably due to strain hardening. Neither matrix softening nor strain hardening occurred for the mortar, so the sharpness was not affected by the cycling.

For metals (steel and aluminum) and mortar, the resistance at the maximum stress of a cycle increased upon cycling, but the reasons were different. For metals, it is due to the oxidation and/or strain hardening. For mortar, it is due to the generation of debris.

The resistance at the minimum stress of a cycle decreased upon cycling for polymer and mortar. Among the metals, the behavior varied. For steel, the resistance at the minimum stress decreased upon cycling at a high stress amplitude of 20.0 MPa (from the third cycle onward), but increased upon cycling at a low stress amplitude of 13.2 MPa; for aluminum and copper, the resistance at the minimum stress increased upon cycling.

Copper differed from steel and aluminum in that its resistance at the maximum stress did not change with cycling and its resistance remained low throughout the cycling. This characteristic is desirable for the use of copper for making electrical connections. Aluminum and steel are less desirable for this application.

4. Conclusion

The metal-metal contact (steel, aluminum and copper), polymer-polymer contact and mortar-mortar contact under cyclic compressive loading below the yield stress were studied by measuring of the contact electrical resistance. For all the contacts, the contact resistance decreased upon compressive loading and increased upon unloading. More contact area was created upon loading, due to local deformation caused by high local stress at the asperities of the interface. The resistance at the minimum stress of a cycle decreased upon load cycling for steel (at a sufficiently high stress amplitude of 20.0 MPa), polymer and mortar, due to plastic deformation, but increased upon load cycling for aluminum and copper, probably due to surface oxidation and/or strain hardening. For steel and aluminum, the resistance at the maximum stress of a cycle increased upon load cycling, probably due to the oxidation and/or strain hardening, and the resistance curve at the maximum stress bent more sharply as cycling progressed, probably due to strain hardening. There was no significant change in the resistance curve for copper upon cycling, probably due to its high electrical conductivity and weak oxide layer. For the polymer, softening occurred at the interface with cycling, probably due to the enhancement of the molecular orientation perpendicular to the stress. For mortar, slight increase of the minimum resistance at the maximum stress was observed as cycling progressed, probably due to debris generation at the interface.

References

1. SHOUKAI WANG and D. D. L. CHUNG, *Composite Interfaces* **6**(6) (1999) 497.
2. ZHEN MEI and D. D. L. CHUNG, *Int. J. Adh. Adh.* **20** (2000) 173.

3. *Idem., ibid.* **20** (2000) 135.
4. PU-WOEI CHEN, XULI FU and D. D. L. CHUNG, *Cem. Concr. Res.* **25**(3) (1995) 491.
5. XULI FU and D. D. L. CHUNG, *ACI Mater. J.* **94**(3) (1997) 203.
6. *Idem., ibid.* **95**(6) (1998) 725.
7. XULI FU, WEIMING LU and D. D. L. CHUNG, *Cem. Concr. Res.* **26**(7) (1996) 1007.
8. XULI FU and D. D. L. CHUNG, *ibid.* **25**(7) (1995) 1391.
9. PU-WOEI CHEN and D. D. L. CHUNG, *Smart Mater. Struct.* **2** (1993) 22.
10. *Metals Handbook*, Vol. 2 (ASM Int., 1990).
11. MELVIN I. KOHAN, "Nylon Plastics" (Wiley, New York, NY, (1973) p. 344.

Received 8 November 1999

and accepted 6 March 2000